Short communication

On the reversibility of hydrogen storage in Ti- and Nb-catalyzed Ca(BH$_4$)$_2$

Jae-Hun Kim, Jae-Hyeok Shim*, Young Whan Cho

Materials Science and Technology Research Division, Korea Institute of Science and Technology, Seoul 136-791, Republic of Korea

ARTICLE INFO

ABSTRACT

The hydrogen sorption properties of calcium borohydride (Ca(BH$_4$)$_2$) catalyzed with a small amount of TiF$_3$, TiCl$_3$, NbF$_5$ or NbCl$_5$ are investigated using thermal analyses and X-ray diffraction. NbF$_5$ exhibits the best performance among all the catalysts; it causes a decrease in the hydrogen desorption temperature which leads to hydrogen absorption at practical temperature and pressure conditions. The hydrogen content of Ca(BH$_4$)$_2$ with NbF$_5$ reaches about 5.0 wt.% after hydrogen absorption at 693 K for 24 h under 90 bar of hydrogen. The main dehydrogenation product of Ca(BH$_4$)$_2$ with NbF$_5$ is a CaH$_{2-x}$F$_x$ solid solution with a CaF$_2$ (C1) structure, while pure Ca(BH$_4$)$_2$ produces CaH$_2$ after hydrogen desorption.

1. Introduction

The development of solid-state hydrogen storage at low and medium temperatures has been recognized as one of the key technologies for hydrogen fuel cell applications. Intensive research efforts have been performed over the last decade to increase the gravimetric and volumetric hydrogen densities of solid-state storage materials [1]. Alkali and alkaline-earth metal borohydrides (tetrahydroborates) such as LiBH$_4$, NaBH$_4$, Mg(BH$_4$)$_2$ and calcium borohydride (Ca(BH$_4$)$_2$), which can be potentially applied for solid-state hydrogen storage, have attracted wide attention because of their high gravimetric and volumetric hydrogen densities [2–31]. Among them, LiBH$_4$ has the highest theoretical hydrogen capacity of 18.5 wt.% when it fully decomposes. It has been known, however, to dehydrogenate to LiH, B and H$_2$, with the release of 13.5 wt.% hydrogen [4,5], and the required pressure and temperature conditions for hydrogenation (hydrogen absorption) are still impractical [7–9].

Although the hydrogen storage capacity of Ca(BH$_4$)$_2$ is lower than that of LiBH$_4$, it has a sufficiently high theoretical capacity (11.6 wt.%) and a lower hydrogen desorption (thermal decomposition) temperature than that of LiBH$_4$ as predicated by thermodynamic analysis based on an ab-initio calculation [29]. In a previous study [20], it was revealed that Ca(BH$_4$)$_2$ desorbs hydrogen in two steps between 620 and 770 K. It decomposes to CaH$_2$ and an unknown intermediate compound in the first-step and to CaH$_2$ and amorphous boron and/or amorphous calcium boride in the second-step.

It has been reported that the performance of sodium alanate (NaAlH$_4$), the most studied complex metal hydride, can be improved dramatically when Ti catalyst is used [32]. Therefore, applying proper catalysts to Ca(BH$_4$)$_2$, which has been demonstrated to exhibit reversible hydrogen storage [21], is the main approach for improving the hydrogen desorption and absorption kinetics under practical temperature and pressure conditions.

In this study, the hydrogen sorption properties of Ti- and Nb-catalyzed Ca(BH$_4$)$_2$ are investigated by thermogravimetric analysis (TGA) and differential scanning calorimetry (DSC). Also, the phase change of Nb-catalyzed Ca(BH$_4$)$_2$ is analyzed by X-ray diffraction (XRD) after hydrogen desorption and absorption.

2. Experimental

Adduct-free Ca(BH$_4$)$_2$ powders were prepared by drying commercial Ca(BH$_4$)$_2$·2THF powders (>96%, Aldrich) under vacuum at 473 K for 5 h. A mixture of adduct-free Ca(BH$_4$)$_2$ and TiF$_3$, TiCl$_3$, NbF$_5$ or NbCl$_5$ (99%, Aldrich) with a molar ratio of 1:0.02 was prepared. One gram of the mixture was charged together with four 12.7 mm and eight 7.9 mm diameter Cr-steel balls into a hardened-steel bowl and sealed with a lid having a Viton O-ring. High-energy ball milling was performed using a Fritsch P7 planetary mill at 500 rpm for 4 h. Apart from ball milling, all materials were handled in an argon-filled glove box (LABstar, MBraun), in which both water vapour and oxygen levels were maintained below 1 ppm.

* Corresponding author. Tel.: +82 2 958 6760; fax: +82 2 958 5379.
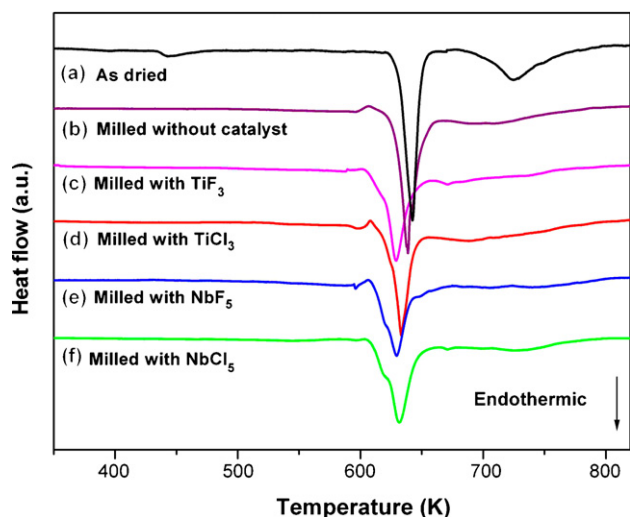*E-mail address:* jhshim@kist.re.kr (J.-H. Shim).

Fig. 1. DSC curves of as-dried $Ca(BH_4)_2$ and $Ca(BH_4)_2$ ball milled with and without catalysts.

Hydrogen desorption and absorption of $Ca(BH_4)_2$ catalyzed with Ti or Nb halides was conducted by the following steps: approximately 200 mg of the milled powder was charged into a stainless-steel tube reactor equipped with a high-pressure valve. Hydrogen desorption was performed in the tube at 693 K for 1 h under a static vacuum. Subsequently, hydrogen absorption was conducted at 623 K for up to 24 h under 90 bar of hydrogen (99.9999%).

The phase composition of the powders was analyzed by XRD (D8 Advance, Bruker AXS) with Cu Kα radiation. A special, air-tight, sample holder was used to prevent any possible reactions between the samples and air during the XRD measurement. The hydrogen desorption behaviour was also analyzed by DSC (DSC 204 F1, Netzsch) and TGA (TG 209 F1, Netzsch). The heating rate was fixed at 5 K min^{-1} and the flow rate of Ar (99.9999%) gas at 50 ml min^{-1} for both DSC and TGA measurements.

3. Results and discussion

The DSC curves of $Ca(BH_4)_2$ with different catalysts are presented in Fig. 1. For comparison, those of as-dried and milled $Ca(BH_4)_2$ specimens are also included. As previously reported [20], two endothermic peaks demonstrate that $Ca(BH_4)_2$ desorbs hydrogen in two steps between 620 and 770 K, as shown in Fig. 1a. The plots in Fig. 1b reveal that the desorption temperature of the sample decreases slightly with peak broadening after ball milling without catalyst. The peak of the second desorption reaction becomes more broadened than the first peak. The decrease in desorption temperature is generally attributed to the fact that lattice defects and reduction of crystallite size produced during ball milling enhance the kinetics of the hydrogen desorption reaction of $Ca(BH_4)_2$, as found for MgH_2 [33]. Fig. 1c–f show that the addition of catalysts further reduces the temperature of the first desorption reaction.

The TGA curve of $Ca(BH_4)_2$ catalyzed with NbF_5 is presented in Fig. 2, together with curves for as-dried and milled $Ca(BH_4)_2$ for comparison. The TGA curves provide information concerning the amount of hydrogen released during hydrogen desorption as well as the desorption temperature range. The inflection points in the TGA curves between 630 and 650 K indicate that the desorption reaction proceeds in two steps, consistent with the DSC curves given in Fig. 1. The results of TGA also agree with those of DSC and reveal that ball milling with and without NbF_5 decreases the

hydrogen desorption temperature; the addition of NbF_5 more effectively decreases the temperature of the first desorption reaction. Although the second endothermic peak in the DSC curve becomes markedly broadened after ball milling as shown in Fig. 1, a considerable weight loss corresponding to the second reaction is clearly observed after ball milling in the TGA curve. After ball milling with NbF_5, the total weight loss, i.e., the amount of desorbed hydrogen, decreases from 9.2 to 8.3 wt.%. This results from a reduction in hydrogen storage capacity due to a chemical reaction between $Ca(BH_4)_2$ and NbF_5 during ball milling. Based on thermodynamic calculations using Thermo-Calc [34], the chemical reaction between $Ca(BH_4)_2$ and NbF_5 is expected to be:

$$4Ca(BH_4)_2 + NbF_5 \rightarrow 2.5CaF_2 + NbB_2 + CaB_6 + 0.5CaH_2 + 15.5H_2\uparrow \tag{1}$$
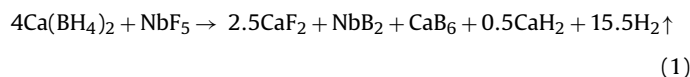
According to this reaction, the total amount of hydrogen that can be desorbed from a mixture of $Ca(BH_4)_2$ and NbF_5 with a molar ratio 1:0.02 is reduced to about 8.3 wt.%, assuming that pure $Ca(BH_4)_2$ desorbs 9.2 wt.% hydrogen, which agrees well with the TGA result. The thermodynamic calculation using Thermo-Calc does not directly provide thermodynamic properties such as changes in enthalpy and Gibbs free energy for reaction (1), since Gibbs free energy data of $Ca(BH_4)_2$ are not available. However, the combination of the Gibb energy data of the other phases with the recent ab-initio calculation of $Ca(BH_4)_2$ by Miwa et al. [23] provides an estimate of the enthalpy change for reaction (1) at about −560 kJ mol^{-1}.

Fig. 3 presents TGA curves of catalyzed $Ca(BH_4)_2$ after hydrogen desorption at 693 K for 1 h under static vacuum and subsequent hydrogen absorption at 623 K for 6 h under 90 bar of hydrogen. It appears that $Ca(BH_4)_2$ milled without catalyst does not absorb under the above conditions, although the detailed data are not presented here. $Ca(BH_4)_2$ with NbF_5 desorbs the most hydrogen (4.6 wt.%), indicating that NbF_5 provides the fastest hydrogen absorption kinetics. NbF_5 exhibits a distinct, two-step, desorption feature with an inflection point at about 620 K, although the weight loss for this first desorption reaction is significantly reduced compared with that for the first desorption reaction in the initial desorption in Fig. 2. By contrast, TiF_3, $TiCl_3$ and $NbCl_3$ do not exhibit the two-step feature, implying that dehydrogenated products with these catalysts fail to reach $Ca(BH_4)_2$ completely during hydrogen absorption. One of the reasons why NbF_5 has the better catalytic effect is that it becomes liquid (mp 350 K) during ball milling and
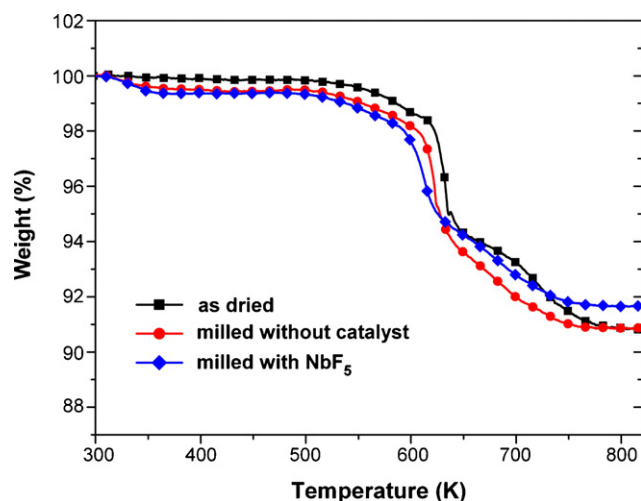

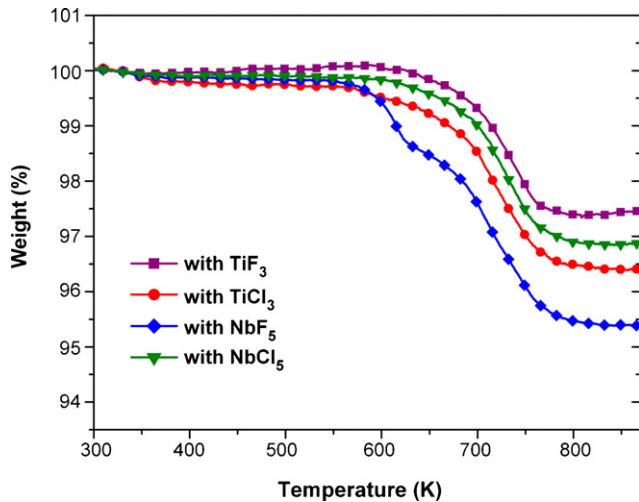**Fig. 2.** TGA curves of as-dried $Ca(BH_4)_2$ and $Ca(BH_4)_2$ ball milled with and without NbF_5.

Fig. 3. TGA curves of catalyzed Ca(BH$_4$)$_2$ after hydrogen absorption at 623 K for 6 h under 90 bar hydrogen.

thus is well dispersed in Ca(BH$_4$)$_2$, as we recently reported for its catalytic effect on the sorption kinetics of MgH$_2$ [35,36].

Fig. 4 gives TGA curves of catalyzed Ca(BH$_4$)$_2$ after hydrogen absorption for 24 h under the same conditions as for Fig. 3. It is found that Ca(BH$_4$)$_2$ with catalysts desorbs 4.1–5.0 wt.% hydrogen, which is larger than the amount of desorbed hydrogen after hydrogen absorption for 6 h (Fig. 3). In particular, TiF$_3$, TiCl$_3$ and NbCl$_5$ catalysts exhibit a considerable improvement in hydrogen storage capacity and start to present two-step hydrogen desorption compared with the desorption after hydrogen absorption for 6 h in Fig. 3. Although NbF$_5$ still exhibits the best results, the amount of desorbed hydrogen after the first hydrogen absorption is 5.0 wt.% at most, which is significantly lower than that from the initial hydrogen desorption (8.3 wt.%). Compared with the TGA curve of the initial desorption in Fig. 2, it is evident that this significant loss in hydrogen storage capacity is caused mainly by less hydrogen desorption in the first-step desorption reaction after the first absorption. This implies that the second-step hydrogen absorption reaction corresponding to the first-step desorption reaction is not completely finished during hydrogen absorption, assuming that the hydrogen absorption reaction follows the desorption reaction path
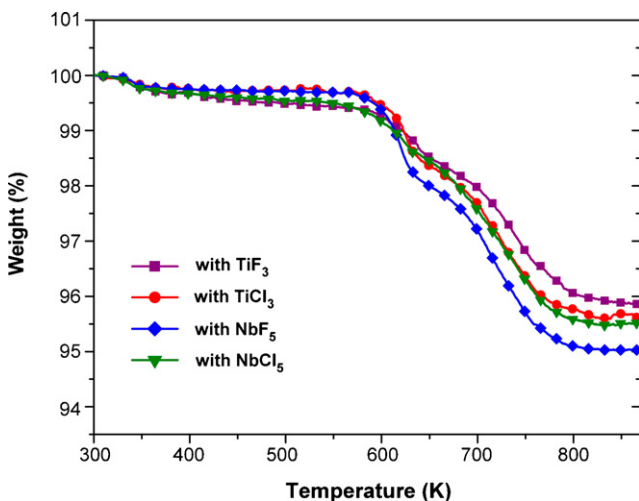

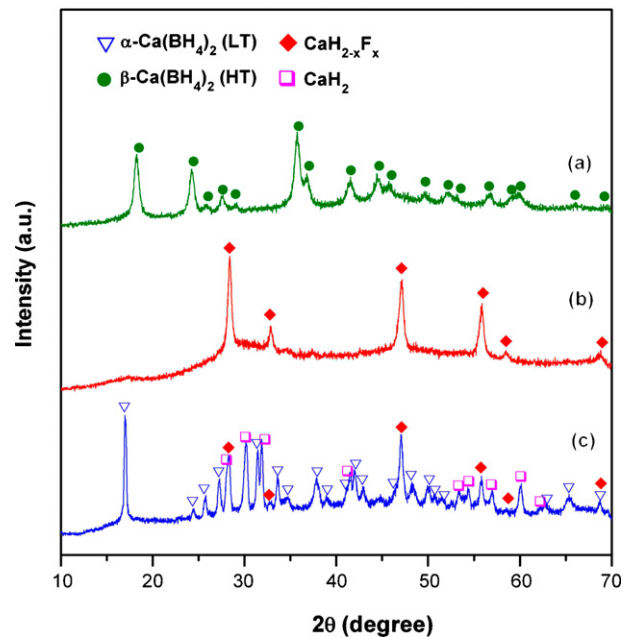**Fig. 4.** TGA curves of catalyzed Ca(BH$_4$)$_2$ after hydrogen absorption at 623 K for 24 h under 90 bar hydrogen.

Fig. 5. XRD patterns of Ca(BH$_4$)$_2$ catalyzed with NbF$_5$: (a) before hydrogen desorption (as-milled); (b) after hydrogen desorption at 693 K under static vacuum; (c) subsequent hydrogen absorption at 623 K for 24 h under 90 bar hydrogen.

in reverse order. The incompletion of the second-step absorption reaction of Ca(BH$_4$)$_2$ is very similar to that of NaAlH$_4$ that also desorbs hydrogen via a two-step reaction [37]. At present, it is not clear whether this feature is associated with either a thermodynamic or a kinetic factor.

Fig. 5 shows XRD patterns of Ca(BH$_4$)$_2$ after milling with NbF$_5$, hydrogen desorption under static vacuum at 693 K and hydrogen absorption under 90 bar of hydrogen at 623 K for 24 h. The as-milled sample (Fig. 5a) has the high temperature phase of Ca(BH$_4$)$_2$ as previously reported [20,21]. Although it is known that CaH$_2$ with an orthorhombic structure (C37) is the main dehydrogenation product of pure Ca(BH$_4$)$_2$ [20], that of Ca(BH$_4$)$_2$ with NbF$_5$ is quite different, as demonstrated in Fig. 5b. The diffraction peaks in Fig. 5b are identified as those of solid solution CaH$_{2-x}$F$_x$ with the same crystal structure as CaF$_2$ (cubic, C1), which Brice et al. [38] have reported. The peaks of CaB$_6$ and NbB$_2$ predicted by the thermodynamic calculation as equilibrium phases, are not clearly seen. CaH$_{2-x}$F$_x$ is distinguished from CaF$_2$ in that it has a relatively strong (2 0 0) peak whereas CaF$_2$ does not, although the two compounds have very similar lattice parameters (a_0 = 5.46 and 5.45 Å for CaF$_2$ and CaH$_{2-x}$F$_x$, respectively). It is quite interesting that a solid solution CaH$_{2-x}$F$_x$ with the CaF$_2$ structure (C1) forms, although the content of H is much higher than that of F in this system. A recent ab-initio calculation [39] concludes that the difference in formation energy of pure CaH$_2$ between the C37 and C1 structures is very small at zero pressure. Therefore, it is possible that the introduction of a small amount of F into CaH$_2$ leads to the reversal of the structural stability of CaH$_2$ between the C37 and C1 structures, i.e., makes the C1 structure more stable than C37. Very recently, Alapati et al. [40] have theoretically shown that cation dopants can improve reaction thermodynamics in destabilized hydride reactions. Thus, this implies that the formation of an anion solid solution such as CaH$_{2-x}$F$_x$ affects reaction thermodynamics, although it is not yet confirmed whether the solid solution can change the thermodynamics in a favourable direction. It is found that Ca(BH$_4$)$_2$ (low-temperature phase) re-forms after hydrogen absorption, as shown in Fig. 5c. In addition to Ca(BH$_4$)$_2$, diffraction peaks of CaH$_2$ and CaF$_{2-x}$H$_x$ are also observed, indicating that complete rehy-

drogenation is not achieved. It is not clear why $CaF_{2-x}H_x$ partially transforms into CaH_2 during hydrogen absorption. High-pressure hydrogen at 90 bar might be one of the reasons for the transformation, although the structural stability at high pressure has still to be examined.

4. Conclusions

$Ca(BH_4)_2$ catalyzed with TiF_3, $TiCl_3$, NbF_5 and $NbCl_5$ has been prepared using high-energy ball milling and its hydrogen sorption properties have been investigated. All the catalysts lower the hydrogen desorption temperature of $Ca(BH_4)_2$ and promote reversible hydrogen storage in $Ca(BH_4)_2$. It is found that $Ca(BH_4)_2$ with NbF_5 absorbs much more hydrogen than that with other halides at 623 K for 24 h under 90 bar of hydrogen. However, the maximum amount of absorbed hydrogen is 5.0 wt.%, which is much lower than that of initially desorbed hydrogen (8.3 wt.%). This loss in hydrogen storage capacity appears to be caused by the incomplete second-step absorption reaction. When $Ca(BH_4)_2$ with NbF_5 desorbs hydrogen, the main de-hydrogenation product is found to be $CaH_{2-x}F_x$ solid solution, not CaH_2. Nevertheless, $CaF_{2-x}H_x$ partially transforms into CaH_2 after hydrogen absorption under high pressure.

Acknowledgement

References

[1] L. Schlapbach, A. Züttel, Nature 414 (2001) 353.
[2] W. Grochala, P.P. Edwards, Chem. Rev. 104 (2004) 1283.
[3] J.-Ph. Soulié, G. Renaudin, R. Černý, K. Yvon, J. Alloys Compd. 346 (2002) 200.
[4] A. Züttel, S. Rentsch, P. Fischer, P. Wenger, P. Sudan, Ph. Mauron, Ch. Emmenegger, J. Alloys Compd. 356–357 (2003) 515.
[5] A. Züttel, P. Wenger, S. Rentsch, P. Sudan, Ph. Mauron, Ch. Emmenegger, J. Power Sources 118 (2003) 1.
[6] S. Orimo, Y. Nakamori, A. Züttel, Mater. Sci. Eng. B 108 (2004) 51.
[7] S. Orimo, Y. Nakamori, G. Kitahara, K. Miwa, N. Ohba, S. Towata, A. Züttel, J. Alloys Compd. 404–406 (2005) 427.
[8] M. Au, A. Jurgensen, J. Phys. Chem. B 110 (2006) 7062.
[9] M. Au, A. Jurgensen, K. Zeigler, J. Phys. Chem. B 110 (2006) 26482.
[10] S. Orimo, Y. Nakamori, N. Ohba, K. Miwa, M. Aoki, S. Towata, A. Züttel, Appl. Phys. Lett. 89 (2006) 021920.
[11] J.K. Kang, S.Y. Kim, Y.S. Han, R.P. Muller, W.A. Goddard III, Appl. Phys. Lett. 87 (2005) 111904.
[12] X.B. Yu, D.M. Grant, G.S. Walker, Chem. Commun. (2006) 3906.
[13] J.J. Vajo, S.L. Skeith, F. Mertens, J. Phys. Chem. B 109 (2005) 3719.
[14] J.J. Vajo, G.L. Olson, Scripta Mater. 56 (2007) 829.
[15] U. Bösenberg, S. Doppiu, L. Mosegaard, G. Barkhordarian, N. Eigen, A. Borgschulte, T.R. Jensen, Y. Cerenius, O. Gutfleisch, T. Klassen, M. Dornheim, R. Bormann, Acta Mater. 55 (2007) 3951.
[16] G. Barkhordarian, T. Klassen, M. Dornheim, R. Bormann, J. Alloys Compd. 440 (2007) L18.
[17] A. Züttel, A. Borgschulte, S. Orimo, Scripta Mater. 56 (2007) 823.
[18] X.B. Yu, Z. Wu, Q.R. Chen, Z.L. Li, B.C. Weng, T.S. Huang, Appl. Phys. Lett. 90 (2007) 034106.
[19] Y.W. Cho, J.-H. Shim, B.-J. Lee, CALPHAD 30 (2006) 65.
[20] J.-H. Kim, S.-A. Jin, J.-H. Shim, Y.W. Cho, J. Alloys Compd., in press, doi:10.1016/j.jallcom.2007.07.097.
[21] J.-H. Kim, S.-A. Jin, J.-H. Shim, Y.W. Cho, Scripta Mater. 58 (2008) 481.
[22] Y. Nakamori, K. Miwa, A. Ninomiya, H. Li, N. Ohba, S. Towata, A. Züttel, S. Orimo, Phys. Rev. B 74 (2006) 045126.
[23] K. Miwa, M. Aoki, T. Noritake, N. Ohba, Y. Nakamori, S. Towata, A. Züttel, S. Orimo, Phys. Rev. B 74 (2006) 155122.
[24] K. Chlopek, C. Frommen, A. Léon, O. Zabara, M. Fichtner, J. Mater. Chem. 17 (2007) 3496.
[25] H.-W. Li, K. Kikuchi, Y. Nakamori, K. Miwa, S. Towata, S. Orimo, Scripta Mater. 57 (2007) 679.
[26] G.L. Soloveichik, M. Andrus, E.B. Lobkovsky, Inorg. Chem. 46 (2007) 3790.
[27] G.L. Soloveichik, Mater. Matters 2 (2007) 11.
[28] 2007 Annual Review Proceedings, U.S. Department of Energy, http://www.hydrogen.energy.gov/annual_review07_storage.html.
[29] D.J. Siegel, C. Wolverton, V. Ozoliņš, Phys. Rev. B 76 (2007) 134102.
[30] S. Orimo, Y. Nakamori, J.R. Eliseo, A. Züttel, C.M. Jensen, Chem. Rev. 107 (2007) 4111.
[31] S.V. Alapati, J.K. Johnson, D.S. Sholl, J. Phys. Chem. B 110 (2006) 8769.
[32] B. Bogdanović, Schwickardi, J. Alloys Compd. 253–254 (1997) 1.
[33] J. Huot, G. Liang, S. Boily, A. Van Neste, R. Schulz, J. Alloys Compd. 293–295 (1999) 495.
[34] http://www.thermocalc.se.
[35] S.-A. Jin, J.-H. Shim, Y.W. Cho, K.-W. Yi, J. Power Sources 172 (2007) 859.
[36] S.-A. Jin, J.-H. Shim, J.-P. Ahn, Y.W. Cho, K.-W. Yi, Acta Mater. 55 (2007) 5073.
[37] N. Eigen, M. Kunowsky, T. Klassen, R. Bormann, J. Alloys Compd. 430 (2007) 350.
[38] J.-F. Brice, A. Courtois, J. Aubry, J. Solid State Chem. 24 (1978) 381.
[39] H. Smithson, C.A. Marianetti, D. Morgan, A. Van der Ven, A. Predith, G. Ceder, Phys. Rev. B 66 (2002) 144107.
[40] S.V. Alapati, J.K. Johnson, D.S. Sholl, Phys. Rev. B 76 (2007) 104108.